



NRL/MR/6170--02-8626

Optical Characterization of Boron-doped Nano-crystalline Diamond

RAFI KALISH

*Institute of Solid State Physics
Haifa, Israel*

JAMES E. BUTLER

*Gas/Surface Dynamics Section
Chemistry Division*

July 25, 2002

Approved for public release; distribution is unlimited.

20020904 011

REPORT DOCUMENTATION PAGE			Form Approved OMB No. 0704-0188	
Public reporting burden for this collection of information is estimated to average 1 hour per response, including the time for reviewing instructions, searching existing data sources, gathering and maintaining the data needed, and completing and reviewing the collection of information. Send comments regarding this burden estimate or any other aspect of this collection of information, including suggestions for reducing this burden, to Washington Headquarters Services, Directorate for Information Operations and Reports, 1215 Jefferson Davis Highway, Suite 1204, Arlington, VA 22202-4302, and to the Office of Management and Budget, Paperwork Reduction Project (0704-0188), Washington, DC 20503.				
1. AGENCY USE ONLY (Leave Blank)		2. REPORT DATE July 5, 2002		3. REPORT TYPE AND DATES COVERED
4. TITLE AND SUBTITLE Optical Characterization of Boron-doped Nano-crystalline Diamond			5. FUNDING NUMBERS BAA 02-001 N0014-02-4028	
6. AUTHOR(S) Rafi Kalish* and James E. Butler				
7. PERFORMING ORGANIZATION NAME(S) AND ADDRESS(ES) Naval Research Laboratory 4555 Overlook Avenue, SW Washington, DC 20375-5320			8. PERFORMING ORGANIZATION REPORT NUMBER NRL/MR/6170--02-8626	
9. SPONSORING/MONITORING AGENCY NAME(S) AND ADDRESS(ES) US Office of Naval Research International Field Office Edison House 223 Old Marylebone Road London NW1 5TH United Kingdom			10. SPONSORING/MONITORING AGENCY REPORT NUMBER	
11. SUPPLEMENTARY NOTES *Institute of Solid State Physics Technion Haifa, Israel				
12a. DISTRIBUTION/AVAILABILITY STATEMENT Approved for public release; distribution is unlimited.			12b. DISTRIBUTION CODE	
13. ABSTRACT (Maximum 200 words) The optical properties of nano-crystalline diamond films and their relation to the presence of boron is the topic of the study undertaken during Prof. Kalish's recent short visit to the Naval Research Laboratory. One of the objectives of the present study was to quantify optical properties of CVD diamond, and correlate them with B and other impurity contents in CVD diamond. To that end, a set of samples grown at NRL was subjected to Raman, PL, Optical and UV as well as IR measurements at NRL, and to SIMS measurements at the Technion.				
14. SUBJECT TERMS Optical properties Nano-crystalline diamond			15. NUMBER OF PAGES 16	
			16. PRICE CODE	
17. SECURITY CLASSIFICATION OF REPORT UNCLASSIFIED	18. SECURITY CLASSIFICATION OF THIS PAGE UNCLASSIFIED	19. SECURITY CLASSIFICATION OF ABSTRACT UNCLASSIFIED	20. LIMITATION OF ABSTRACT UL	

CONTENTS

1. GENERAL BACKGROUND	1
2. EXPERIMENTAL	3
2.1 Growth of Nano-crystalline CVD Diamond Layers	3
2.2 Evaluation Methods	3
3. RESULTS	4
4. DISCUSSION	6

"Optical characterization of Boron-doped nano-crystalline diamond"

Professor Rafi Kalish
Institute of Solid State Physics
Technion
Haifa Israel

Dr. James E. Butler
Gas/Surface Dynamics Section, Code 6174
Chemistry Division
Naval Research Laboratory
Washington DC 20375

1. General background:

Diamond is a material with outstanding mechanical, chemical, optical and electronic properties. It is thus no surprise that fundamental and applied research on the synthesis of bulk and layered diamond, on understanding of diamond properties and on the search for applications for this unique material has attracted much interest in the last decade. In particular Japan has, and still is, investing huge amounts of money into national efforts devoted to the various aspects of diamond-related technologies. These efforts are now starting to yield results as diamond now finds commercial applications, mainly as a material to be used in extremely high frequency devices, required for communication, as chemically inert electrodes, to be used in electrochemistry, as very robust windows transparent to a wide part of the ultra-violet, visible and infra-red spectrum ,and as hard coatings.

The huge potential in the use of diamond as a material for electronic applications, which promises unique performances thanks to diamond's special physical and chemical properties has not yet found wide application, mainly because of problems related to the synthesis of "electronic grade" diamond layers with the required purity, doping levels and carrier mobilities. Also, the realization of stable ohmic contacts to doped diamond has not been satisfactorily achieved. Ion-implantation, which is a key technology in the realization of all modern Si based devices, is still problematic when applied to diamond

because of the meta-stability of diamond with respect to graphite. Most recently a way was devised how to prepare very thin, B doped and undoped, diamond layers with nano-scale grains. These thin films may find many applications due to their high integrity, even when very thin (of several tens of nano-meters thickness).

The optical properties of this novel diamond film and its relation to the presence of boron have not been studied so far, they are the topic of the study undertaken by Butler and Kalish during Kalish's recent visit at NRL. One of the objectives of the present study, not yet completed, was to quantify optical properties of CVD diamond and correlate them with B and other impurity contents in CVD diamond.

To that end, identical samples were subjected to Raman, PL, Optical and UV as well as IR absorption measurements at NRL, and to SIMS measurements at the Technion.

The excellent Secondary Ion Mass Spectrometry (SIMS) facilities available to Kalish at the Technion's Solid State Institute, offers detailed assessment of impurity concentrations in the diamond, information that is essential for understanding the origin of electrical and optical properties of the sample under study.

During the visit of Kalish to NRL, growth of thin nano-crystalline diamond layers under different growth conditions and H_2S gas content was achieved. These layers, when removed from the Si substrate could be subjected to optical investigations, the results of which are described here. Identically grown samples, but on insulating (fused silica) substrates were also produced. These are currently subjected to electrical measurements at Kalish's laboratory at the Technion (conductivity as function of temperature, and if possible Hall effect as function of temperature).

In a different project growth and characterization of homo-epitaxial layers grown in the presence of H_2S and in the unavoidable presence of some B contamination, changing gas composition and substrate temperatures, was carried out. This part of the research is not yet completed; and may be the subject of a future report.

2. Experimental:

2.1 Growth of Nano-crystalline CVD diamond layers

Numerous nano-crystalline diamond layers were grown in a standard 1.5 kW Astex reactor on Si, following the pre-treatment procedure developed at NRL which was proven to lead to dense nucleation, ca. $> 10^{11}/\text{cm}^2$, followed by the growth of nano-crystalline diamond layers. The main growth parameters which were varied were substrate temperature and gas mixture. In the latter, either unintentional (residual) B, intentional B (from di-borane) and intentional S (from H_2S) dopants were used.

The samples were always thinner than 3 microns, more typically 500 nm.

Part of the sample was removed from the Si substrate by wet etching, leaving a self-supporting membrane for optical (transmission) evaluation.

The details of the samples which were analyzed here are given in **table 1** arranged in increasing B content (see B/C gas phase column and [B] SIMS column).

2.2 Evaluation methods:

2.2.1 Raman spectroscopy

Raman spectra were taken at room temperature, using a Renishaw Model 100 confocal spectrometer excited by the 488nm Ar ion laser line and scanning the range of 200 to 3000 cm^{-1} . Diamond films supported on Si were probed, so that the underlying first and second order Si lines, the diamond first order 1332 cm^{-1} line, as well as the D and G lines of graphitic carbon, and the Fano resonance between the B related ionization continuum and the diamond phonon, could be monitored. The laser spot size was ca. 1 micron diameter and the probe depth was limited to 2-3 microns.

2.2.2. Photoluminescence.

The same system used for the Raman spectroscopy was employed to monitor the Photoluminescence (PL) from the samples. A wide range of photon energies from 480 nm to 800 nm was scanned.

2.2.3 Infra-Red absorption spectroscopy.

A Thermo-Nicolet Nexus model 870 Fourier transform infrared system was used to measure the IR absorption at RT. A free standing membrane was positioned in the beam, and transmission measurements were performed. The background atmospheric absorption was automatically corrected.

Three kinds of measurements were performed: (1) perpendicular beam incidence, (2) Brewster angle beam incidence, and (3) Brewster angle incidence with p polarized light. The first measurement was used to obtain the film thickness when Fabry Perot interference fringes were observed, whereas the Brewsters angle measurements were performed to suppress the interference fringes.

2.2.4 Optical and UV absorption spectroscopy:

UV, visible, and near IR absorption measurements were made using a Varian Cary 5E dual beam spectrometer with the membrane samples oriented at normal incidence to the beam.

2.2.5 Secondary ion Mass spectrometry (SIMS)

SIMS measurements on selected samples were performed at the Technion, using a CAMECA 4F instrument. Both sample thickness (at the probed spot), absolute B content and its depth profile, as well as the presence of some other impurities were evaluated. The nitrogen signal contains contributions from CO, ethylene, and hydrocarbon fragments and is not representative of the true nitrogen contaminants in the film.

3. Results:

Below we concentrate on results from a selected set of CVD grown nano-crystalline diamond having different B content.

Table 1 lists the growth parameters of the samples, their thickness (as evaluated from interference patterns obtained during growth and as obtained by the optical transmission measurements-see below) and their B content, as determined by SIMS.

3.1.1 Raman spectroscopy

Figure 1a-1h shows Raman spectra of diamond films with increasing B content (as determined by SIMS). Also shown, for comparison (Fig 1a), is the Raman spectrum of a synthetic type Ib (Sumitomo) diamond.

The main features that should be noted are: (i) the well-known diamond peak at 1332 cm^{-1} and its width; (ii) the broad peak at about 1600 cm^{-1} which signifies the presence of non- sp^3 bonded carbon; (iii) the resonance about the diamond 1332 cm^{-1} peak (Fano Resonance) most notable in figure 1(h), and (iv) the broad photoluminescence background. In some case the Raman first and second order modes of the Si substrate are observed at 521 and 980 cm^{-1} .

3.1.2 Photoluminescence

Figures 2a-2h shows PL spectra obtained from the differently B doped nano-crystalline layers. Also shown, for comparison (fig 2a) is a PL spectrum of a CVD film which predominantly contains N (hence the zero phonon lines of the N-V and $(\text{N-V})^-$ centers and their phonon replicas are visible).

For the B doped layers the reduction in the absolute PL intensity and the broad luminescence at about 650 nm should be noted. Also seen are the Raman features of the Si substrate and the diamond films (between 500 and 550 nm 's).

3.1.3 Infra-red spectroscopy

Figures 3a-3g shows the absorbance in the IR with the membranes at normal incidence to the optical path and corrected for film thickness. The one phonon absorption at about 1300 cm^{-1} , due to impurities breaking the local symmetry, is noticeable in the higher doped samples. Also, the increased absorbance over the near IR and extending into the IR and visible wave-length ranges with increasing B content should be noted.

3.1.4 Near IR, Visible and UV spectroscopy

Figures 4a-4g show the absorbance of the films in the range of $200\text{-}3000\text{ nm}$ measured at normal incidence and corrected for film thickness. The raw data are dominated by interference fringes due to internal reflection in the membranes. The increased

absorbance, with higher boron doping, should be noted. This absorbance in the IR and far red spectral regions gives the films the well-known bluish tint of heavily B doped diamond.

3.1.5 Secondary ion mass spectrometry (SIMS)

Figures 5a to 5d show the secondary ion mass spectrometry (SIMS) of samples with increasing levels of boron doping. The nitrogen levels reported in the figure are upper limits and probably are dominated by contributions from CO, ethylene, and other hydrocarbon ions of mass within the resolution of the instrument.

4. Discussion:

The samples studied were thin layers composed of densely packed nano-crystallites of diamond. As such, their properties may significantly deviate from those of bulk boron doped single crystalline diamond.

The analysis performed did not consider this possible difference in the material, although one could imagine that the extremely large surface to volume ratio of nano crystals might have an effect on the properties of the B containing samples. All diagnostic methods employed did not have high enough resolution to permit probing of individual crystallites. Hence physical properties averaged over many crystallites and over many different facets were measured.

The major finding of this work, which somewhat signifies the present data from previously published work on optical properties of B containing diamond, is the lack of any distinct features in the spectra. The reason for this may well be the average nature of the data taken, which has smeared out all sharp lines due to stain, grain boundaries or growth defects.

The other peculiarity of the data is in the fact that only when extremely heavily doped (as determined by SIMS) did features characteristic for heavily doped diamond emerge. This is particularly evident in the Raman spectra which show the Fano resonance only when the doping level is as high as 5×10^{20} B/cm³. At B concentrations lower by less than factor

of 10 (which for homogeneously distributed impurities is reflected by only an increase of the average distance between impurities of less than a factor of 2) did these features become nearly unobservable. The appearance of the Fano resonance with increasing doping level is well understood. It is due to the broadening of the B related acceptor levels and their merging into a band, the width of which is increasing with doping level. The wider this band, the higher the overlap of B related levels with the Raman phonon-related levels, giving rise to the appearance of the resonance.

The fact that this occurs only at very high B concentrations may hint that much of the B detected by SIMS is not located inside the diamond crystallites, where it acts as an acceptor, but much of it may be located on the peripheries of the crystals.

The fact that the photoluminescence is quenched for the heavily doped samples may be caused by both the level overlap or by the presence of many defect related non-radiative recombination centers.

The same applies to the increased absorption noticed for the heavily doped samples.

It is interesting to study the role of diamond crystal size on the optical effects noticed here, as some smooth transition from the properties of the finely granular material to single crystalline should be expected.

Table 1:

Run Date	H2 flow	CH4 flow	B2H6 flow 0.1% in H2	H2S flow 0.518% in H2	Press	Microwave Power	Substrate Temp.	thickness	C/H gas phase	B/C gas phase	Technion SIMS
	sccm	sccm	sccm	sccm	torr	Watts	C	microns	atom %	atom ppm	
4/10/02 (N3S0011)	900	3	0	0	15	800	800	0.53	0.166	0	
4/15/02 (N3S0014)	900	3	0	12	15	800	800	0.53	0.166	0	
10/5/01	900	3	0	0	15	800	750	1.57	0.166	0	
10/7/01	900	8	0	0	15	800	750	3.3	0.437	0	1.00E+20
11/1/01	900	9	0.6	0	15	800	830	1.31	0.490	133	3.00E+20
12/7/01	900	3	1	0	15	800	750	0.53	0.165	667	5.00E+20
3/20/01	500	1.5	1	0	15	800	800	2	0.148	1333	1.50E+21

Figure 1: Raman Spectra of various diamond films as a function of boron dopants (see text).

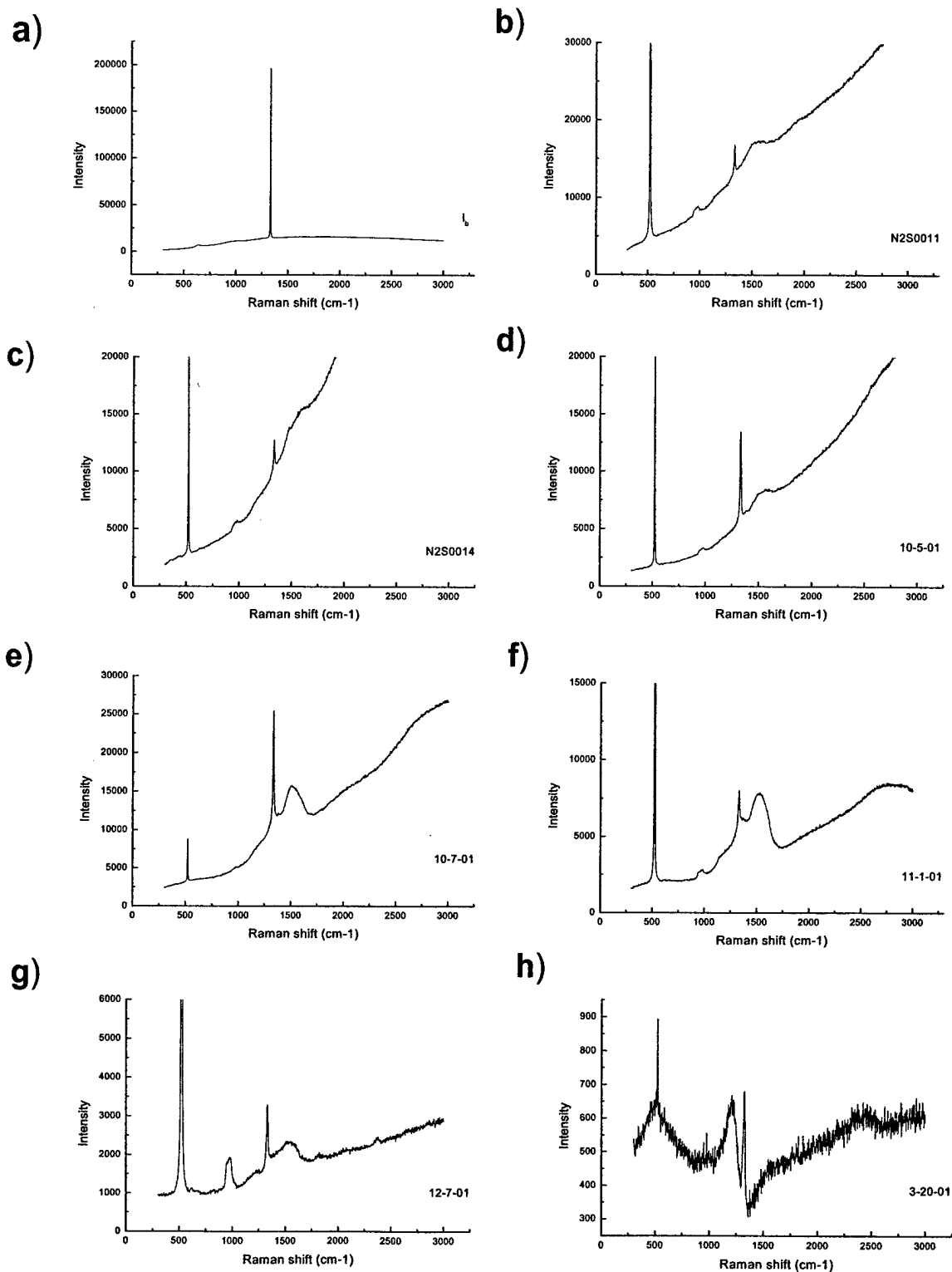


Figure 2: Photoluminescence spectra of various diamond films as a function of boron dopants (see text).

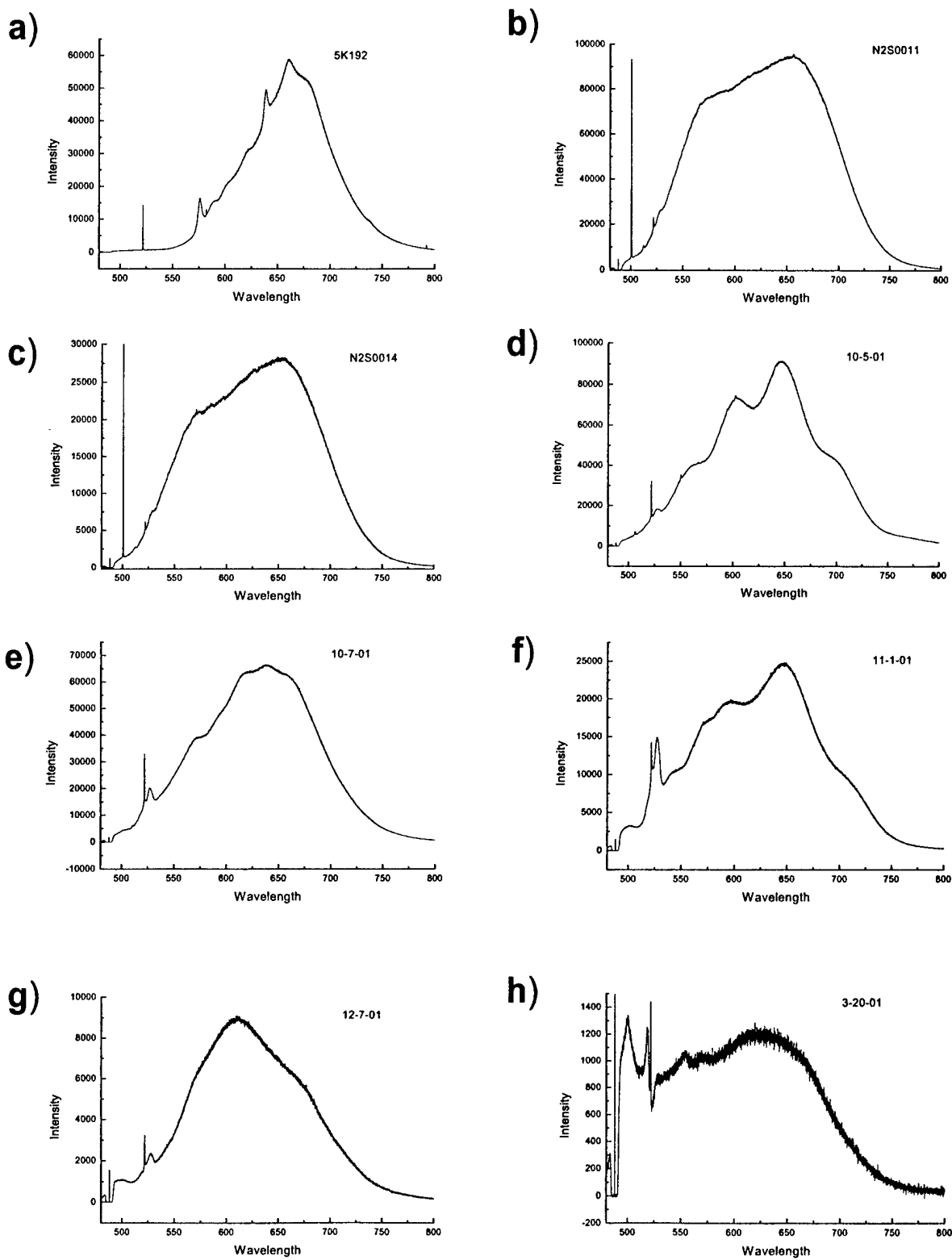


Figure 3: Infrared Spectra at normal incidence of various diamond films as a function of boron dopants (see text).

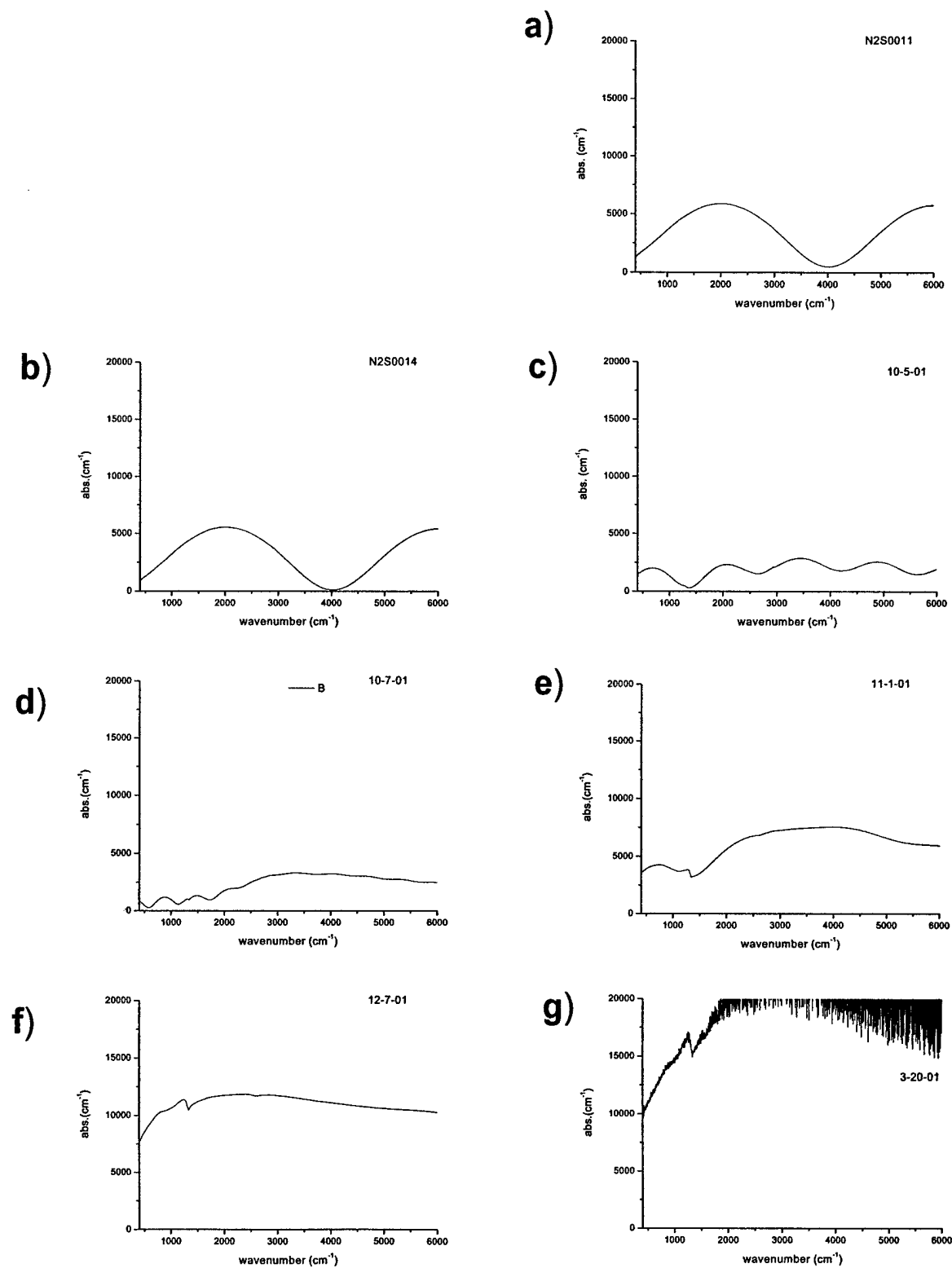


Figure 4: UV-visible-near IR spectra at normal incidence of various diamond films as a function of boron dopants (see text).

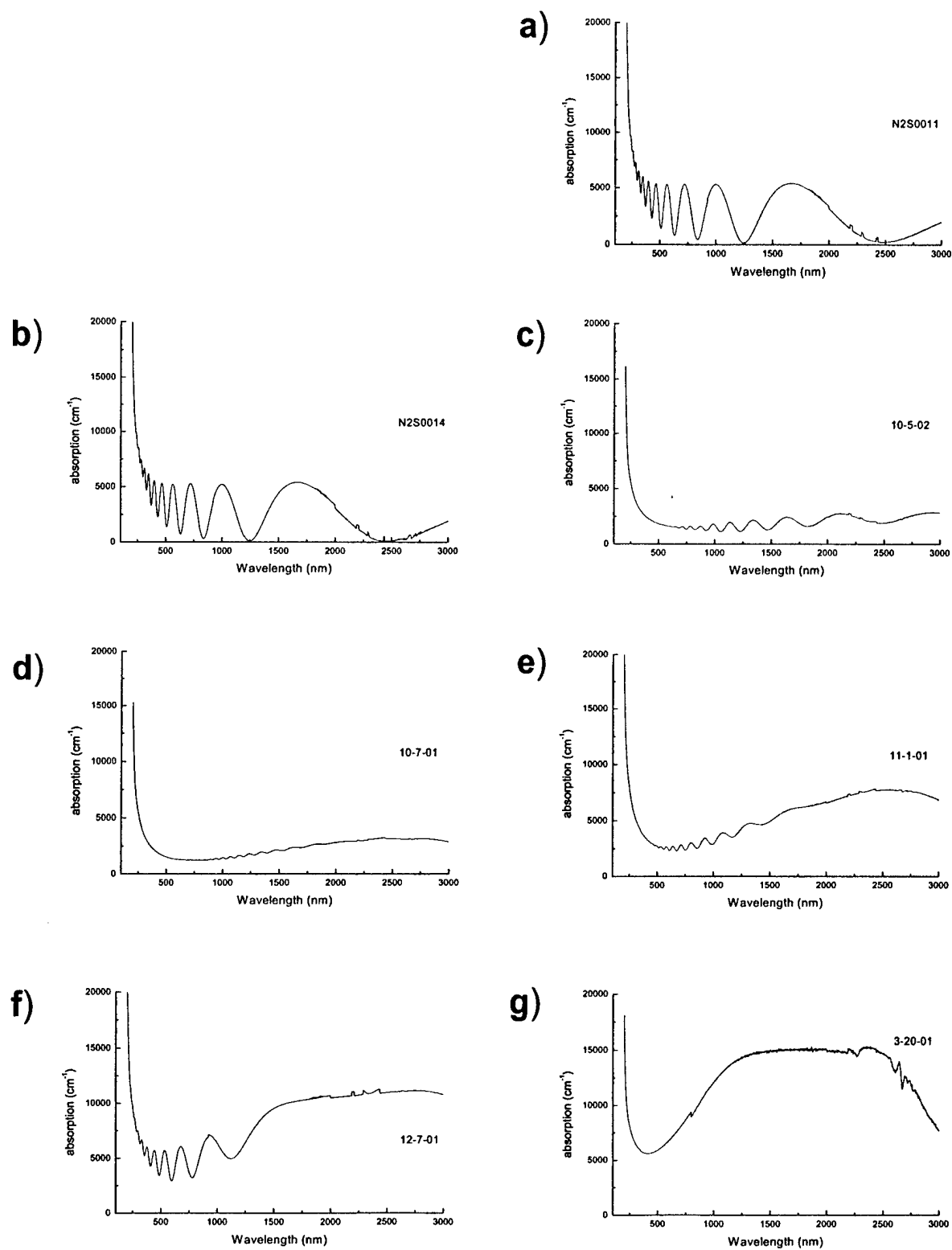
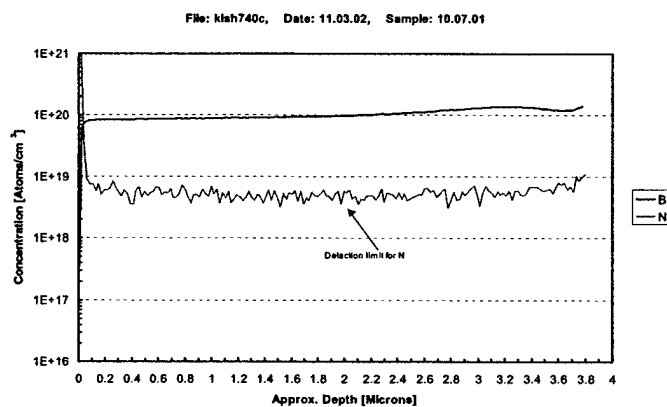
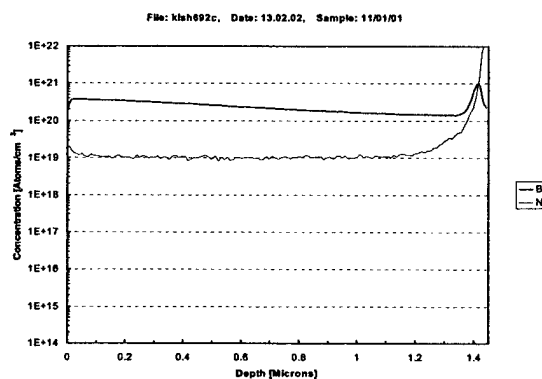


Figure 5: SIMS data of various diamond films as a function of boron dopants (see text).

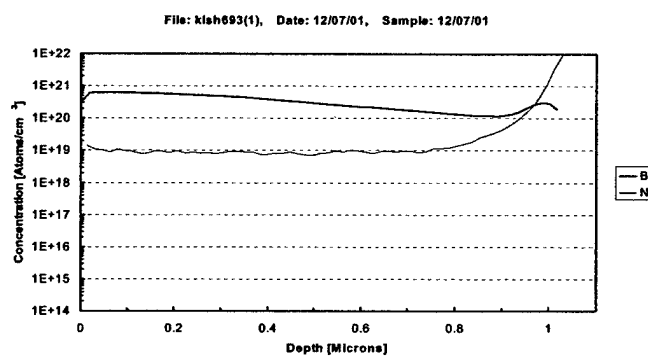
a)



b)



c)



d)

